

# High-harmonic generation driven by temporal-mode quantum states of light

Juan M. González-Monge<sup>\*</sup> and Johannes Feist<sup>†</sup>

*Departamento de Física Teórica de la Materia Condensada, Universidad Autónoma de Madrid, E-28049 Madrid, Spain  
Condensed Matter Physics Center (IFIMAC), Universidad Autónoma de Madrid, E-28049 Madrid, Spain and  
Instituto Nicolás Cabrera (INC), Universidad Autónoma de Madrid, E-28049 Madrid, Spain*

(Dated: December 9, 2025)

We develop a theoretical framework for high-harmonic generation (HHG) driven by quantum states of light based on a temporal-mode expansion of the electromagnetic field. This approach extends previous single plane-wave mode treatments to realistic pulse configurations, resolving conceptual inconsistencies arising from non-normalizable infinite plane waves and establishing consistency between analytical and numerical methods. We derive a correction factor that quantifies deviations from the single-mode approximation and show that it remains below  $10^{-4}$  for intensities typical of HHG ( $\sim 10^{14}$  W/cm<sup>2</sup>). This result confirms that free-space HHG driven by any quantum state of light is accurately described by averaging semi-classical calculations over the Husimi distribution, with no observable genuine quantum effects. The absence of such effects is attributed to the large photon numbers ( $\sim 10^{11}$ ) required to reach HHG intensities in free space, which render quantum fluctuations negligible. We discuss nanophotonic environments with ultrasmall mode volumes as potential platforms where few-photon strong-field processes could exhibit genuine quantum signatures.

## I. INTRODUCTION

In the last few years, there has been increasing interest in the quantum features of light in the context of attosecond science and strong-field physics [1–11]. An important motivation for this has been the development of bright squeezed vacuum (BSV) sources [12–14], which enable the use of nonclassical driving pulses for strong-field physics [15–21]. Studying the process of high-harmonic generation (HHG), Gorlach et al. developed a theoretical framework demonstrating that, under reasonable approximations, the HHG signal driven by quantum states of light can be obtained by averaging several *semi-classical* calculations with classical driving fields [15]. The weights in the averaging are determined by the Husimi quasiprobability distribution  $Q(\alpha) = \langle \alpha | \rho_F | \alpha \rangle$ , where  $\rho_F$  is the density operator of the electromagnetic field and  $|\alpha\rangle$  is a coherent state, with the classical field amplitude directly proportional to the coherent state amplitude  $\alpha$ .

This prescription implies that HHG driven by any quantum field can be equivalently reproduced by a statistical average over a collection of simulations with classical pulses, indicating that there can be no “quantum advantage” in HHG. The increased cutoff observed for quantum states of light such as BSV is simply due to the fact that the electric field amplitude fluctuates strongly in these states. Consequently, for a given average intensity, much higher peak intensities are included in the statistical distribution. A collection of classical pulses with different peak intensities (and the same intensity distribution) would provide the same enhancement in the cutoff.

However, the derivation in Ref. [15] relies on several assumptions that may not hold in all situations. In particular, the driving field is assumed to be in a single-mode plane-wave state even in the limit of infinite volume, which means that it fills all of space and is, in principle, not in a normalizable state. The derivation depends on the fact that the formal normalization prefactor  $\propto V^{-1/2}$  vanishes in the free-space limit  $V \rightarrow \infty$ , where  $V$  is the quantization volume. Furthermore, the numerical calculations do not actually employ an infinite plane wave, but rather a finite one with a well-defined temporal profile with a total duration of 25 laser cycles. The numerical and analytical results are thus not fully consistent with each other.

In the current work, we resolve these issues by extending the framework developed in Ref. [15] to the case of a driving field that is not in a single plane-wave state, but in a temporal mode—i.e., a wavepacket that is localized in time and space. Generalizing the results obtained in Ref. [15] to this more realistic scenario, we obtain an analytical result almost identical to the one given there, with a correction factor that can be shown to be extremely close to unity for realistic driving fields containing many photons.

Our results also close a small loophole in the argument given above: Since the “most classical” state of light, a coherent state, is itself a quantum state with non-zero width in the Husimi distribution (i.e., with unavoidable quantum noise), even HHG driven by a coherent field must include some averaging over different classical field amplitudes. Consequently, non-classical states of light (whose Husimi functions have features narrower than a unit width) could still potentially exhibit genuine quantum effects in HHG. Our results demonstrate explicitly that these effects are negligible for all realistic driving fields in free space, precluding the observation of genuine quantum effects unless extremely strong subwavelength

<sup>\*</sup> [juanmanuel.gonzalezm@estudiante.uam.es](mailto:juanmanuel.gonzalezm@estudiante.uam.es)

<sup>†</sup> [johannes.feist@uam.es](mailto:johannes.feist@uam.es)

confinement of the driving field is achieved such that the intensities required for HHG are reached with a small number of photons.

The manuscript is structured as follows: We first introduce the theoretical framework in Sec. II, where we derive the main result of this work. In Sec. III, we present numerical results for HHG driven by different quantum states of light and compare the results obtained using the single-mode and temporal-mode frameworks. Finally, we summarize our findings and their implications in Sec. IV.

## II. THEORETICAL FRAMEWORK

We treat a single-electron atom interacting with the quantized electric field within the framework of non-relativistic quantum electrodynamics, employing the dipole (long-wavelength) approximation in the Power-Zienau-Woolley picture. The Hamiltonian describing the system consists of three terms [22]:

$$H = H_A + H_F + \vec{d}_A \cdot \vec{E}(\vec{r}_0) \quad (1)$$

where  $H_A = \frac{\vec{p}^2}{2m} + U(\vec{r})$  is the atomic Hamiltonian describing an electron with momentum  $\vec{p}$  moving in the potential  $U(\vec{r})$  of the nucleus (assumed fixed in space at  $\vec{r} = \vec{r}_0 = \vec{0}$ ),  $H_F = \sum_{\ell} \hbar \omega_{\ell} a_{\ell}^{\dagger} a_{\ell}$  is the free-field Hamiltonian, and  $\vec{d}_A = e\vec{r}$  is the atomic dipole operator. The electric field operator  $\vec{E}(\vec{r})$  expanded in a plane-wave basis is given by

$$\vec{E}(\vec{r}) = \sum_{\ell} \vec{f}_{\ell}(\vec{r}) a_{\ell} + \text{H.c.} \quad (2a)$$

$$\vec{f}_{\ell}(\vec{r}) = i\vec{e}_{\ell} \sqrt{\frac{\hbar \omega_{\ell}}{2V \epsilon_0}} e^{i\vec{k}_{\ell} \cdot \vec{r}}, \quad (2b)$$

where  $\ell = (\vec{k}_{\ell}, \sigma_{\ell})$  is a combined index running over both the wave vector  $\vec{k}_{\ell}$  and the polarization  $\sigma_{\ell}$  (with two possible polarization states per wave vector) for compact notation,  $\vec{e}_{\ell}$  is the polarization vector,  $a_{\ell}$  and  $a_{\ell}^{\dagger}$  are the annihilation and creation operators, respectively, and  $V$  is the quantization volume. The frequency  $\omega_{\ell}$  for each mode is given by  $\omega_{\ell} = c|\vec{k}_{\ell}|$ .

We write a sum over the mode index for simplicity of notation—in the continuous ( $V \rightarrow \infty$ ) limit, this sum will become a mixture of integrals and sums. Furthermore, in principle the atomic Hamiltonian should contain a polarization self-energy term that formally diverges but partially cancels the equally divergent contribution of the vacuum field to the light-matter interaction, producing a logarithmically divergent result that gives the (small) Lamb shift after proper regularization [23]. We do not explicitly include the polarization self-energy as we do not calculate the vacuum correction to the energy levels.

For any initial (mixed or pure) state, the von Neumann equation

$$i\hbar \frac{\partial \rho(t)}{\partial t} = [H, \rho(t)], \quad (3)$$

governs the time evolution of the density matrix  $\rho(t)$  describing both the atom and the light field. For convenience, we switch to the interaction picture with respect to the field Hamiltonian  $H_F$  via the transformation  $\rho(t) \rightarrow e^{-\frac{i}{\hbar} H_F t} \rho(t) e^{\frac{i}{\hbar} H_F t}$ . The equation to solve in the interaction picture is

$$i\hbar \frac{\partial \rho(t)}{\partial t} = [H_o(t), \rho(t)], \quad (4)$$

where  $H_o(t) = H_A + \vec{d} \cdot \vec{E}(\vec{r}, t)$ , and the electric field now takes the form

$$\vec{E}(\vec{r}, t) = e^{-\frac{i}{\hbar} H_F t} \vec{E}(\vec{r}) e^{\frac{i}{\hbar} H_F t} = \sum_{\ell} \vec{f}_{\ell}(\vec{r}, t) a_{\ell} + \text{H.c.} \quad (5a)$$

$$\vec{f}_{\ell}(\vec{r}, t) = \vec{f}_{\ell}(\vec{r}) e^{-i\omega_{\ell} t} = i\vec{e}_{\ell} \sqrt{\frac{\hbar \omega_{\ell}}{2V \epsilon_0}} e^{i(\vec{k}_{\ell} \cdot \vec{r} - \omega_{\ell} t)}. \quad (5b)$$

### A. Temporal mode basis

We now perform a unitary transformation from the plane-wave basis to a basis of wavepackets or “temporal modes” [24],  $a_{\ell} = \sum_{\nu} U_{\ell\nu} b_{\nu}$ , described by operators  $b_{\nu}$ . Since the transformation is unitary, the resulting basis again describes independent bosons, i.e.,  $[a_{\ell}, a_{\ell'}^{\dagger}] = \delta_{\ell, \ell'}$  implies  $[b_{\nu}, b_{\nu'}^{\dagger}] = \delta_{\nu, \nu'}$ . Inserting this transformation into the electric field operator yields

$$\vec{E}(\vec{r}, t) = \sum_{\nu} \vec{g}_{\nu}(\vec{r}, t) b_{\nu} + \text{H.c.}, \quad (6)$$

where we have defined the temporal mode functions  $\vec{g}_{\nu}(\vec{r}, t) = \sum_{\ell} U_{\ell\nu} \vec{f}_{\ell}(\vec{r}, t)$ . We note that the unitarity of  $U_{\ell\nu}$  implies a normalization condition for the mode fields  $\vec{g}_{\nu}(\vec{r}, t)$ .

In the following, we assume that the quantum driving field is always in the same temporal mode, which we denote by the index  $\nu = p$ . This assumption replaces the single plane-wave state assumption in Ref. [15] and decouples the state of the light field from the formal free-space limit  $V \rightarrow \infty$ . It also resolves the conceptual problem of calculating the action of an infinitely extended (always-on) light field on a single atom, since we can choose  $\vec{g}_p(\vec{0}, t) = 0$  for  $t < 0$ , and makes the numerical simulations consistent with the analytical results. Our assumption implies that in the initial state, only the mode  $b_p$  will have non-zero photon population. The associated mode function  $\vec{g}_p(\vec{r}, t)$  thus contains the complete information about the temporal shape and frequency content of the pulse, while the quantum distribution of the light is contained within the quantum state of mode  $p$  and probed by the operator  $b_p$ .

We note that while we only treat the case of a single temporal driving mode in the current work, the formalism can be straightforwardly extended to multiple modes.

## B. Time evolution

We follow a procedure similar to that presented by Goriach et al. [15] to rewrite (under appropriate approximations) the general solution for the system density matrix in a form that is amenable to numerical solution.

Before the action of the light pulse, the electromagnetic field and atomic states are not entangled. Consequently, the initial density matrix  $\rho(0)$  can be represented as the tensor product of the density matrices for the atom and the electromagnetic field:  $\rho(0) = \rho_A(0) \otimes \rho_F(0)$ , where  $\rho_A(0)$  is the atomic density matrix and  $\rho_F(0)$  is the field density matrix. The atom is assumed to be initially in its ground state,  $\rho_A(0) = |g\rangle\langle g|$ .

To describe the initial state  $\rho_F(0)$  of the field, we first review some key concepts regarding quasi-probability distributions. The density matrix for a light mode  $\nu$  can be written in terms of the positive  $P$  representation and the projection operator  $\Lambda(\alpha, \beta^*)$  [25]:

$$\rho_\nu = \int d^2\alpha d^2\beta P_\nu(\alpha, \beta^*) \Lambda_\nu(\alpha, \beta^*), \quad (7)$$

where the projection operator is  $\Lambda_\nu(\alpha, \beta^*) = \frac{|\alpha\rangle\langle\beta|}{\langle\beta|\alpha\rangle}$ ,  $|\alpha\rangle$  and  $\langle\beta|$  denote coherent states with complex number parameters  $\alpha$  and  $\beta$ , and coherent state matrix elements satisfy  $\langle\beta|\alpha\rangle = e^{-\frac{1}{2}(|\alpha|^2 + |\beta|^2 - 2\alpha^*\beta)}$ . The positive  $P$  representation takes the form  $P_\nu(\alpha, \beta^*) = \frac{1}{4\pi^2} e^{\frac{-|\alpha-\beta|^2}{4}} \left\langle \frac{\alpha+\beta}{2} \left| \rho_\nu \right| \frac{\alpha+\beta}{2} \right\rangle = \frac{1}{4\pi} e^{\frac{-|\alpha-\beta|^2}{4}} Q_\nu\left(\frac{\alpha+\beta}{2}\right)$ , where  $Q_\nu(\alpha) = \langle\alpha|\rho_\nu|\alpha\rangle$  is the Husimi distribution containing the quasi-probability distribution of light states in the coherent state basis. Note that the bras and kets here are written without an explicit mode index for compactness; they are to be understood as states in the Hilbert space of the mode  $\nu$  of interest.

Since only the mode associated with index  $p$  is initially active and all other modes are in the vacuum state, the density matrix of the electromagnetic field at  $t = 0$  can be written as

$$\rho(0) = \int d^2\alpha d^2\beta P(\alpha, \beta^*) \frac{|\alpha\rangle\langle\beta|}{\langle\beta|\alpha\rangle} \otimes \prod_{\nu \neq p} |0_\nu\rangle\langle 0_\nu|, \quad (8)$$

where  $\alpha$  and  $\beta$  are implicitly assumed to refer to mode  $p$  from now on. Using the fact that the von Neumann equation Eq. (4) is linear, and that  $P(\alpha, \beta^*)$  is independent of time, it is possible to define  $\rho_{\alpha\beta}(t)$  such that it satisfies

$$i\hbar \frac{\partial \rho_{\alpha\beta}(t)}{\partial t} = [H_o(t), \rho_{\alpha\beta}(t)], \quad (9)$$

where  $\rho_{\alpha\beta}(0) = |g\rangle\langle g| \otimes |\alpha\rangle\langle\beta| \otimes \prod_{\nu \neq p} |0_\nu\rangle\langle 0_\nu|$ . The time-dependent version  $\rho_{\alpha\beta}(t)$  is implicitly defined from the complete density matrix operator via

$$\rho(t) = \int d^2\alpha d^2\beta \frac{P(\alpha, \beta^*)}{\langle\beta|\alpha\rangle} \rho_{\alpha\beta}(t). \quad (10)$$

Following steps analogous to those in Ref. [15], and given in more detail in Appendix A, the problem can be rewritten such that it is only necessary to solve a Schrödinger equation:

$$i\hbar \frac{\partial |\psi_\alpha(t)\rangle}{\partial t} = H_\alpha(t) |\psi_\alpha(t)\rangle, \quad (11a)$$

$$H_\alpha(t) = H_A + \vec{d}_A \cdot (\vec{E} + \vec{E}_\alpha(t)) \quad (11b)$$

where the initial condition is  $|\psi_\alpha(0)\rangle = |g\rangle \otimes \prod_\nu |0_\nu\rangle$ , and the new term contains a classical field in mode  $p$ ,  $\vec{E}_\alpha(t) = \vec{g}_p(\vec{r}, t)\alpha + \text{c.c.}$

Using the same assumptions and approximations as in Refs. [2, 9], the electromagnetic field state can be written as a product of coherent states. This corresponds to a mean-field approximation for the back-action of the atom on the electromagnetic field, or equivalently to including only the coherent fields produced by atomic dipole oscillations and neglecting incoherent contributions due to fluctuations. The coherent contributions dominate when spontaneous emission is not important, as is the case for the HHG spectrum. Under these approximations,  $|\psi_\alpha(t)\rangle$  may be written as a tensor product:

$$|\psi_\alpha(t)\rangle = |\phi_\alpha(t)\rangle \otimes \prod_\ell |\gamma_\ell^\alpha\rangle. \quad (12)$$

The first term  $|\phi_\alpha(t)\rangle$  satisfies the Schrödinger equation for the atom and its interaction with the classical field:

$$i\hbar \frac{\partial |\phi_\alpha(t)\rangle}{\partial t} = (H_A + \vec{d} \cdot \vec{E}_\alpha(t)) |\phi_\alpha(t)\rangle. \quad (13)$$

The second term, consisting of the product of  $|\gamma_\ell^\alpha\rangle$ , represents the coherent states of light written in the original plane-wave basis where the frequency is well-defined. The coherent state amplitudes can be expressed in terms of the Fourier transform of the expectation value of the atomic dipole moment operator.

$$\begin{aligned} \gamma_\ell^\alpha &= -\frac{1}{\hbar} \vec{d}_\alpha(\omega_\ell) \cdot \vec{f}_\ell(\vec{0}) \\ \vec{d}_\alpha(\omega) &= \int_{-\infty}^t e^{i\omega\tau} \langle\phi_\alpha(t)|\vec{d}|\phi_\alpha(t)\rangle d\tau. \end{aligned} \quad (14)$$

We are interested in the asymptotic state at  $t \rightarrow \infty$  when all HHG processes have concluded. For simplicity of notation, we thus drop most explicit time arguments in the following.

The density matrix operator is then given by

$$\begin{aligned} \rho &= \int d^2\alpha d^2\beta \frac{P(\alpha, \beta^*)}{\langle\beta|\alpha\rangle} |\phi_\alpha\rangle\langle\phi_\beta| \\ &\quad \times \left( D(\alpha) \prod_{\ell_1 \ell_2} |\gamma_{\ell_1}^\alpha\rangle\langle\gamma_{\ell_2}^\beta| D^\dagger(\beta) \right), \end{aligned} \quad (15)$$

where  $D(\alpha) = e^{\alpha b^\dagger - \alpha^* b}$  is the displacement operator for the temporal mode of the pulse  $p$ . To apply this operator, we express it as a product of displacement operators in the plane-wave basis and use that the action of

a displacement operator on a coherent state is given by  $D(\alpha)|\beta\rangle = e^{(\alpha\beta^* - \alpha^*\beta)/2}|\alpha + \beta\rangle$ . The pulse mode operator can be expressed through the unitary transformation as  $b = \sum_\ell c_\ell a_\ell$ , where we introduce  $c_\ell = U_{\ell p}^*$  for simplicity of notation. Due to the unitarity of  $U$ , these coefficients fulfill  $\sum_\ell |c_\ell|^2 = 1$ . This gives  $D(\alpha) = \prod_\ell D_\ell(\alpha_\ell)$  with  $\alpha_\ell = c_\ell \alpha$ . As a consequence,

$$D(\alpha) \prod_\ell |\gamma_\ell^\alpha\rangle = \prod_\ell D_\ell(\alpha_\ell) |\gamma_\ell^\alpha\rangle \\ = \prod_\ell e^{i\varphi_\ell} |\gamma_\ell^\alpha + \alpha_\ell\rangle = \prod_\ell |\Gamma_\ell^\alpha\rangle, \quad (16)$$

where  $\varphi_\ell = \frac{1}{2i}(\alpha_\ell \gamma_\ell^{\alpha*} - \alpha_\ell^* \gamma_\ell^\alpha)$ , and the states  $|\Gamma_\ell^\alpha\rangle$  have been defined implicitly with the exponential factor. Eq. (15) can thus be rewritten as

$$\rho = \int d^2\alpha d^2\beta \frac{P(\alpha, \beta^*)}{\langle\beta|\alpha\rangle} |\phi_\alpha\rangle\langle\phi_\beta| \prod_{\ell_1 \ell_2} |\Gamma_{\ell_1}^\alpha\rangle\langle\Gamma_{\ell_2}^\beta|. \quad (17)$$

### C. HHG spectrum

Having obtained the density matrix describing the system, we can now calculate the HHG spectrum by considering the expectation value of the electromagnetic energy:

$$\varepsilon = \sum_\ell \text{Tr}(\hbar\omega_\ell a_\ell^\dagger a_\ell \rho) = \sum_\ell \varepsilon_\ell. \quad (18)$$

With  $\rho$  from Eq. (17),  $\varepsilon_\ell$  becomes

$$\varepsilon_\ell = \hbar\omega_\ell \int d^2\alpha d^2\beta \frac{P(\alpha, \beta^*)}{\langle\beta|\alpha\rangle} \langle\phi_\beta|\phi_\alpha\rangle \\ \times \prod_{\ell_1 \ell_2} \langle\Gamma_{\ell_2}^\beta| a_\ell^\dagger a_\ell |\Gamma_{\ell_1}^\alpha\rangle. \quad (19)$$

As coherent states are eigenstates of the annihilation operator, and states of different modes are orthogonal, we get

$$\prod_{\ell_1 \ell_2} \langle\Gamma_{\ell_2}^\beta| a_\ell^\dagger a_\ell |\Gamma_{\ell_1}^\alpha\rangle = \Gamma_\ell^{\beta*} \Gamma_\ell^\alpha \prod_{\ell_1} \langle\Gamma_{\ell_1}^\beta|\Gamma_{\ell_1}^\alpha\rangle. \quad (20)$$

The coherent state amplitudes  $\Gamma_\ell^\alpha$  are sums of two contributions,  $\Gamma_\ell^\alpha = \gamma_\ell^\alpha + \alpha_\ell$ . Additionally, with the previous definition of the phase exponentials,

$$\langle\Gamma_{\ell_1}^\beta|\Gamma_{\ell_1}^\alpha\rangle = e^{i(\varphi_{\ell_1}^\alpha - \varphi_{\ell_1}^\beta)} \langle\gamma_{\ell_1}^\beta + \beta_{\ell_1}|\gamma_{\ell_1}^\alpha + \alpha_{\ell_1}\rangle. \quad (21)$$

Using the previously mentioned overlap for coherent states  $\langle\beta|\alpha\rangle$  and the expression for  $P(\alpha, \beta^*)$  given earlier, Eq. (19) can be expanded as

$$\varepsilon_\ell = \hbar\omega_\ell \int d^2\alpha d^2\beta \frac{e^{-\frac{|\alpha - \beta|^2}{4}}}{4\pi} Q\left(\frac{\alpha + \beta}{2}\right) \langle\phi_\beta|\phi_\alpha\rangle$$

$$\times \left( \gamma_\ell^\alpha \gamma_\ell^{\beta*} + \alpha_\ell \gamma_\ell^{\beta*} + \beta_\ell^* \gamma_\ell^\alpha + \alpha_\ell \beta_\ell^* \right) \\ \times \exp \left\{ \sum_{\ell_1} \left[ \gamma_{\ell_1}^{\alpha*} \gamma_{\ell_1}^\beta - \frac{1}{2} |\gamma_{\ell_1}^\alpha|^2 - \frac{1}{2} |\gamma_{\ell_1}^\beta|^2 \right. \right. \\ \left. \left. + \alpha^* c_{\ell_1}^* (\gamma_{\ell_1}^\beta - \gamma_{\ell_1}^\alpha) - \beta c_{\ell_1} (\gamma_{\ell_1}^\beta - \gamma_{\ell_1}^\alpha)^* \right] \right\}. \quad (22)$$

Our interest lies in the high-harmonic spectrum, such that only terms with  $\omega_\ell \gg \omega_0$  are of interest. For these terms, we can assume  $c_\ell \approx 0$ , as the driving laser pulse is concentrated within some bandwidth around the main frequency  $\omega_0$ , and has no frequency components in the high-harmonic range. As such, the contribution of  $\alpha_\ell \gamma_\ell^{\beta*} + \beta_\ell^* \gamma_\ell^\alpha + \alpha_\ell \beta_\ell^*$  in the last expression can be ignored. Furthermore, we perform a change of variables

$$\begin{cases} \alpha_m = \frac{1}{2}(\alpha + \beta), \\ \delta\alpha = \frac{1}{2}(\alpha - \beta), \end{cases} \quad (23)$$

which lets us rewrite the expression for the energy spectrum as

$$\varepsilon_\ell = \hbar\omega_\ell \int d^2\alpha_m d^2\delta\alpha \frac{e^{-|\delta\alpha|^2}}{\pi} Q(\alpha_m) \langle\phi_\beta|\phi_\alpha\rangle \gamma_\ell^\alpha \gamma_\ell^{\beta*} \\ \times \exp \left\{ \sum_{\ell_1} \left[ \gamma_{\ell_1}^{\alpha*} \gamma_{\ell_1}^\beta - \frac{1}{2} |\gamma_{\ell_1}^\alpha|^2 - \frac{1}{2} |\gamma_{\ell_1}^\beta|^2 \right. \right. \\ \left. \left. + \alpha^* c_{\ell_1}^* (\gamma_{\ell_1}^\beta - \gamma_{\ell_1}^\alpha) - \beta c_{\ell_1} (\gamma_{\ell_1}^\beta - \gamma_{\ell_1}^\alpha)^* \right] \right\}, \quad (24)$$

where  $\alpha = \alpha_m + \delta\alpha$  and  $\beta = \alpha_m - \delta\alpha$  are to be understood as implicit functions of the new variables.

Since the integrand contains a Gaussian in  $\delta\alpha$ , the main contributions to the integral will come from values of  $\delta\alpha$  close to zero. At the same time, HHG only occurs in intense pulses, which typically corresponds to large photon numbers, implying  $|\alpha_m| \gg |\delta\alpha|$ . Expanding all terms except for the Gaussian to lowest order in the small variable  $|\delta\alpha|/\alpha_m$  then corresponds to a “diagonal” approximation  $\alpha \approx \beta \approx \alpha_m$ , and the remaining Gaussian can be integrated analytically. The energy spectrum in this approximation simplifies to

$$\varepsilon_\ell^{\text{diag}} = \hbar\omega_\ell \int d^2\alpha_m d^2\delta\alpha \frac{e^{-|\delta\alpha|^2}}{\pi} Q(\alpha_m) \|\phi_{\alpha_m}\|^2 |\gamma_\ell^{\alpha_m}|^2 \\ = \frac{\omega_\ell^2}{2\epsilon_0 V} \int d^2\alpha_m Q(\alpha_m) |\vec{e}_\ell \cdot d_{\alpha_m}(\omega_\ell)|^2. \quad (25)$$

In the last step, we used that the atom wavefunction  $|\phi_\alpha\rangle$  is normalized and employed the expression for  $\gamma_\ell^\alpha$  in terms of  $d_\alpha(\omega)$  from Eq. (14). Next, we take the free-space limit  $V \rightarrow \infty$ , corresponding to  $\sum_\ell \rightarrow \frac{V}{(2\pi)^3 c^3} \int_0^\infty d\omega \omega^2 \sum_\sigma \int d\Omega$ , and group all modes with the same frequency, giving the spectrum

$$\frac{d\varepsilon^{\text{diag}}}{d\omega} = \frac{\omega^4}{6\pi^2 \epsilon_0 c^3} \int d^2\alpha Q(\alpha) |d_\alpha(\omega)|^2. \quad (26)$$

The diagonal approximation thus reduces exactly to the result obtained in the single-mode approximation in Ref. [15]. We next study the accuracy of this approximation. Grouping all the terms that do not depend on  $\delta\alpha$  outside the respective integral from Eq. (24), the energy  $\varepsilon_\ell$  can be written as

$$\varepsilon_\ell = \hbar\omega_\ell \int d^2\alpha_m C_\ell(\alpha_m) Q(\alpha_m) |\gamma_\ell(\alpha_m)|^2, \quad (27)$$

where  $C_\ell(\alpha_m)$  is a correction factor that does not depend on the state of the light pulse and is given by

$$C_\ell(\alpha_m) = \int d^2\delta\alpha \frac{e^{-|\delta\alpha|^2}}{\pi} \frac{\gamma_\ell^\alpha \gamma_\ell^{\beta*}}{|\gamma_\ell(\alpha_m)|^2} \langle \phi_\beta | \phi_\alpha \rangle \times \exp \left\{ \sum_{\ell_1} \left[ \gamma_{\ell_1}^\alpha \gamma_{\ell_1}^\beta - \frac{1}{2} |\gamma_{\ell_1}^\alpha|^2 - \frac{1}{2} |\gamma_{\ell_1}^\beta|^2 + \alpha^* c_{\ell_1}^* (\gamma_{\ell_1}^\beta - \gamma_{\ell_1}^\alpha) - \beta c_{\ell_1} (\gamma_{\ell_1}^\beta - \gamma_{\ell_1}^\alpha)^* \right] \right\}, \quad (28)$$

The validity of the diagonal approximation then depends on how much  $C_\ell(\alpha_m)$  differs from unity for the values of  $\alpha_m$  that contribute significantly to the Husimi distribution  $Q(\alpha_m)$  for a given driving field. To calculate this correction factor explicitly, we express  $\gamma$ ,  $\alpha$ , and  $\beta$  in terms of the physical dipole moments and electric fields.

The first term in Eq. (28) can be written as

$$\frac{\gamma_\ell^\alpha \gamma_\ell^{\beta*}}{|\gamma_\ell(\alpha_m)|^2} = \frac{(\vec{d}_\alpha(\omega_\ell) \cdot \vec{e}_\ell)(\vec{d}_\beta^*(\omega_\ell) \cdot \vec{e}_\ell)}{|\vec{d}_{\alpha_m}(\omega_\ell) \cdot \vec{e}_\ell|^2} = \frac{d_\alpha(\omega_\ell) d_\beta^*(\omega_\ell) \sin^2(\theta)}{|d_{\alpha_m}(\omega_\ell)|^2 \sin^2(\theta)} = \frac{d_\alpha(\omega_\ell) d_\beta^*(\omega_\ell)}{|d_{\alpha_m}(\omega_\ell)|^2}. \quad (29)$$

where  $\theta$  is the polar angle of  $\vec{k}_\ell$ , and we used that  $\vec{d} \propto \hat{z}$  since we assume driving light that is linearly polarized along the  $z$  axis, such that only terms  $\ell$  with polarization components along the  $z$ -axis have non-zero components. We now turn to the terms inside the exponential in Eq. (28). The continuous limit for the first term gives

$$t_1(\alpha, \beta) = \sum_{\ell_1} \left( \gamma_{\ell_1}^\alpha \gamma_{\ell_1}^\beta - \frac{1}{2} |\gamma_{\ell_1}^\alpha|^2 - \frac{1}{2} |\gamma_{\ell_1}^\beta|^2 \right) = \frac{1}{4(2\pi)^3 \hbar c^3 \epsilon_0} \int_0^\infty d\omega \omega^3 \int d\Omega \sin^2(\theta) (2d_\alpha^*(\omega) d_\beta(\omega) - |d_\alpha(\omega)|^2 - |d_\beta(\omega)|^2) = \frac{1}{12\pi^2 \hbar c^3 \epsilon_0} \int_0^\infty d\omega \omega^3 (2d_\alpha^*(\omega) d_\beta(\omega) - |d_\alpha(\omega)|^2 - |d_\beta(\omega)|^2) \quad (30)$$

where the sum over polarizations uses a basis where only one of the two polarizations has a  $z$ -component, and the solid angle integral gives  $\int d\Omega \sin^2(\theta) = \frac{8}{3}\pi$ . The second term of the exponential can be rewritten in terms of the Fourier transform of the driving electric field (see Appendix B for details), giving

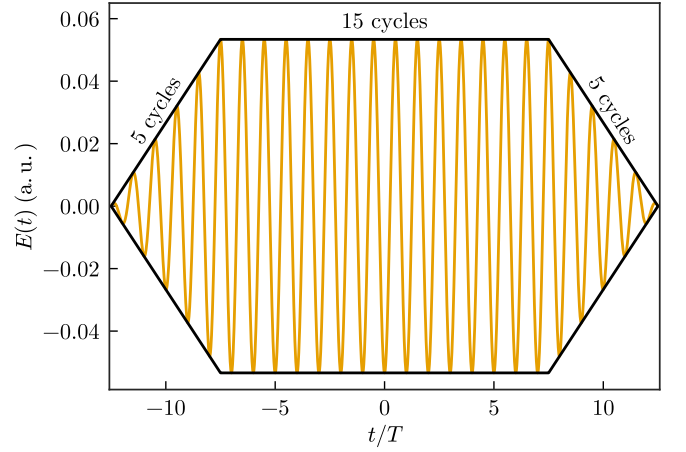


FIG. 1. Illustration of the electric field pulse shape  $E(t)$  used, given by a single-frequency carrier wave modulated with a flat-top pulse envelope. The envelope rises linearly over 5 cycles, becomes constant for 15 cycles, and then decreases linearly over 5 cycles.  $E(t)$  is given in atomic units for a peak intensity of  $I_0 = 10^{14}$  W/cm<sup>2</sup> and  $t$  in units of the period  $T = \frac{2\pi}{\omega_0}$ .

$$t_2(\alpha, \beta) = \sum_{\ell_1} \left[ \alpha^* c_{\ell_1}^* (\gamma_{\ell_1}^\beta - \gamma_{\ell_1}^\alpha) - \beta c_{\ell_1} (\gamma_{\ell_1}^\beta - \gamma_{\ell_1}^\alpha)^* \right] = \frac{1}{\sqrt{2\pi\hbar}} \int_0^\infty d\omega \left[ \vec{E}_\alpha^{+*}(\omega) \cdot (\vec{d}_\beta(\omega) - \vec{d}_\alpha(\omega)) - \vec{E}_\beta^+(\omega) \cdot (\vec{d}_\beta^*(\omega) - \vec{d}_\alpha^*(\omega)) \right], \quad (31)$$

where  $\vec{E}_\alpha^+(\omega)$  is the positive-frequency part of the Fourier transform of the driving electric field with coherent parameter  $\alpha$ .

The complete expression for the correction factor can then be written as

$$C_\ell(\alpha_m) = \int d^2\delta\alpha \frac{e^{-|\delta\alpha|^2}}{\pi} f_\ell(\alpha_m, \delta\alpha), \quad (32a)$$

$$f_\ell(\alpha_m, \delta\alpha) = \frac{d_\alpha(\omega_\ell) d_\beta^*(\omega_\ell)}{|d_{\alpha_m}(\omega_\ell)|^2} f_{\text{ov}}(\alpha_m, \delta\alpha), \quad (32b)$$

$$f_{\text{ov}}(\alpha_m, \delta\alpha) = \langle \phi_\beta | \phi_\alpha \rangle e^{t_1(\alpha, \beta) + t_2(\alpha, \beta)}, \quad (32c)$$

where  $f_{\text{ov}}(\alpha_m, \delta\alpha)$  does not depend on the mode index  $\ell$ , and  $\alpha = \alpha_m + \delta\alpha$  and  $\beta = \alpha_m - \delta\alpha$  are implicit functions of  $\alpha_m$  and  $\delta\alpha$ . The diagonal approximation is equivalent to assuming  $f_\ell(\alpha_m, \delta\alpha) \approx 1$ .

### III. RESULTS

In this section, we apply the developed theory to calculate the HHG spectrum and analyze the correction factor  $C_\ell(\alpha_m)$  to evaluate the validity of the diagonal approximation. As mentioned above, we assume that the driving light is in a single temporal mode,  $\vec{E}_d(\vec{r}, t) =$



$\vec{g}_p(\vec{r}, t)b_p + \text{H.c.}$  To facilitate comparison, we assume that the temporal profile of the pulse mode at the atom position is the same flat-top laser pulse as used in the numerical simulations in Ref. [15], given by

$$\vec{g}_p(\vec{r} = 0, t) = \hat{z}E_{1,p}F_{\text{flat}}(t)e^{-i\omega_0 t} \quad (33a)$$

$$F_{\text{flat}}(t) = \begin{cases} 1 & |t| \leq \frac{1}{2}T_f \\ 1 - \frac{|t| - \frac{1}{2}T_f}{T_r} & \frac{1}{2}T_f < |t| \leq T_r + \frac{1}{2}T_f \\ 0 & |t| > T_r + \frac{1}{2}T_f \end{cases} \quad (33b)$$

where  $F_{\text{flat}}(t)$  is the linear flat-top pulse envelope, the carrier wavelength is  $\lambda_0 = 800$  nm, corresponding to a period  $T = \lambda_0/c$  and central frequency  $\omega_0 = 2\pi/T$ , and  $T_r = 5T$  and  $T_f = 15T$  are the durations of the linear ramp-on and flat parts of the pulse, respectively. This flat-top pulse is represented in Fig. 1.

To ensure the  $b_p$  and  $b_p^\dagger$  operators follow the commutation relations described previously, the electric field must be properly normalized. To accomplish this, the full spatial shape of the mode function  $\vec{g}_p(\vec{r}, t)$  needs to be defined, not just its value at the position of the atom. We assume that it corresponds to a laser pulse propagating in free space along the  $x$ -axis with a flat transverse profile with cross-sectional area  $A = 1 \mu\text{m}^2$ , corresponding to a relatively well-focused beam. The temporal shape given by the flat-top envelope described above then also determines the spatial profile along the  $x$ -axis. The normalization procedure, detailed in Appendix C, then gives

$$E_{1,p} = \sqrt{\frac{\hbar\omega_0}{2\varepsilon_0 V_{\text{eff}}}}, \quad (34)$$

where  $V_{\text{eff}} \approx 18.34\lambda_0 A$  is the effective pulse quantization volume for the pulse parameters above. The (temporal) peak intensity  $I$  of the pulse is then given by

$$I = 2c\varepsilon_0 E_{1,p}^2 \langle b_p^\dagger b_p \rangle = I_{1,p} \langle b_p^\dagger b_p \rangle = I_{1,p} |\alpha_p|^2, \quad (35)$$

where  $I_{1,p} = c\hbar\omega_0/V_{\text{eff}}$  is the peak intensity per photon in the pulse mode,  $\langle b_p^\dagger b_p \rangle$  is the photon number operator, and the equality  $\langle b_p^\dagger b_p \rangle = |\alpha_p|^2$  applies for coherent states. For the pulse parameters used here, we obtain values of  $E_{1,p} \approx 30,911$  V/m and  $I_{1,p} \approx 507.26$  W/cm<sup>2</sup>. This means that peak intensities of  $I_{\text{HHG}} \approx 10^{14}$  W/cm<sup>2</sup> as required for HHG will only occur if the Husimi distribution  $Q(\alpha_m)$  contains non-negligible contributions at  $|\alpha_m|^2 \approx I_{\text{HHG}}/I_{1,p} \approx 2 \times 10^{11}$ , corresponding to  $|\alpha_m| \approx 4.4 \times 10^5$ .

The large photon numbers needed for HHG imply that the diagonal approximation is expected to be accurate, as only values of  $\delta\alpha$  close to unity are expected to contribute significantly to the integral in  $C_\ell(\alpha_m)$  due to the suppression by the Gaussian factor  $e^{-|\delta\alpha|^2}$ , so that  $\delta\alpha/\alpha_m \sim 10^{-5} \ll 1$  holds for all relevant contributions. The expression for  $f_\ell(\alpha_m, \delta\alpha)$  then suggests that its value will be close to unity, implying  $C_\ell(\alpha_m) \approx 1$ , for which the temporal-mode expansion for the energy spectrum, Eq. (27), reduces to the single-mode formula, Eq. (25).

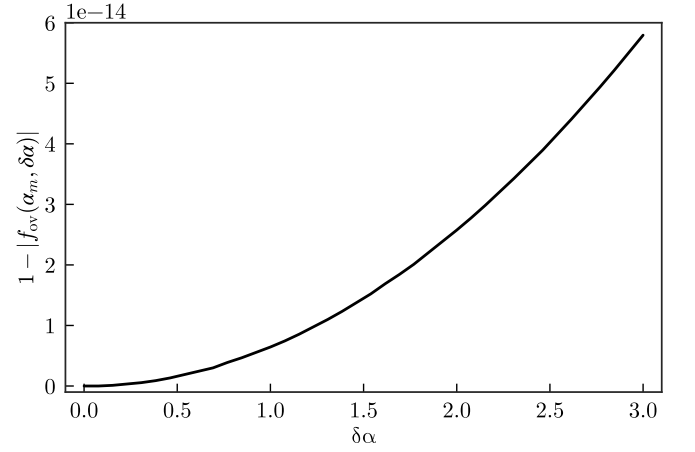


FIG. 2. Deviation of the frequency-independent overlap factor  $f_{\text{ov}}$  from unity over a range of  $\delta\alpha$  large enough to avoid complete Gaussian suppression.

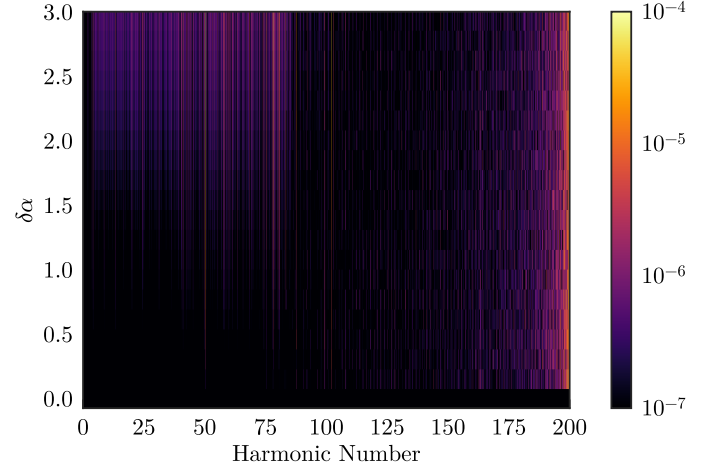


FIG. 3. Evaluation of the difference  $1 - |f_l(\alpha_m, \delta\alpha)|$ , represented by the colorbar, as a function of  $\omega$  and  $\delta\alpha$ . Vertical bands are a consequence of numerical noise.

To quantify the accuracy of this approximation, we next evaluate the correction factors  $f_\ell(\alpha_m, \delta\alpha)$  and  $f_{\text{ov}}(\alpha_m, \delta\alpha)$  explicitly. We do so by solving the Schrödinger equation described in Eq. (13) and computing the expectation value of the dipole acceleration  $\langle \ddot{d} \rangle(t) = -\langle \frac{dV}{dz} \rangle + E(t)$  and its Fourier transform. To maintain easy comparison with Ref. [15], we solve the dynamics using the same 1D model atom characterized by a soft Coulomb potential with the same ionization potential  $I_p$  as neon:

$$H_A = -\frac{1}{2} \frac{d^2}{dz^2} + V(z); \quad V(z) = -\frac{1}{\sqrt{z^2 + a^2}}, \quad (36)$$

where  $a = 0.8160 r_B$  is chosen such that  $I_p = 0.7924$  Hartree. Setting  $\alpha_m = \sqrt{I_{\text{HHG}}/I_{1,p}}$ , we show the mode-independent term  $f_{\text{ov}}(\alpha_m, \delta\alpha)$  in Fig. 2. As can be seen, its deviation from unity is completely neg-

ligible in this range, on the order of  $10^{-14}$ . The full correction factor  $f_\ell(\alpha_m, \delta\alpha)$  is shown in Fig. 3. As expected, the deviation increases for larger values of  $\delta\alpha$ , but it remains below  $10^{-4}$  within the entire range considered. Furthermore, the largest corrections, seen as narrow vertical bands in the figure, are mostly due to numerical noise near minima of the Fourier transform of the dipole expectation value  $|d_{\alpha_m}(\omega_\ell)|^2$ .

These results indicate that the diagonal approximation  $C_\ell(\alpha_m) \approx 1$  is indeed justified for the values of  $\alpha_m$  relevant for HHG production within the integral over  $Q(\alpha_m)$ , such that the single-mode approximation used in Ref. [15] is accurate for HHG with pulses in arbitrary quantum states in free space. For the diagonal approximation to break down, one would need to consider situations where much smaller values of  $\alpha_m$  are relevant, such that small deviations  $\delta\alpha$  can have a significant effect. This observation reinforces the general idea that many quantum effects in light-matter interaction require the photon number to be small, such that the quantized nature of light is relevant. While this is not possible for HHG in free space, where the effective pulse volume is on the order of  $\lambda_0^3$ , it could potentially occur in nanophotonic environments where the mode volume is strongly reduced, such that the same peak intensity can be reached with much smaller photon numbers. For  $\lambda_0 = 800$  nm, the number of photons required to reach  $I_{\text{HHG}} = 10^{14}$  W/cm<sup>2</sup> is given by  $I_{\text{HHG}}/I_{1,p} = 13.4 \text{ V[nm}^3]$ . This implies that for the smallest mode volumes predicted in plasmonic nanogap picocavities, on the order of  $V \sim 1 \text{ nm}^3$  [26, 27], few-photon HHG could potentially be within the reach of experiment, and quantum effects could become significant.

For completeness, we next calculate the high harmonic spectrum for the same quantum light states considered in [15]: coherent, Fock, thermal, and bright-squeezed vacuum (BSV). The same mean intensity  $I = 10^{14}$  W/cm<sup>2</sup> is considered for all the associated Husimi distributions of these light states [28]. The HHG spectrum is shown in Fig. 4, where the amplitude of the response is plotted against the frequency (in terms of the harmonic number  $\omega/\omega_0$ ). Since the correction factor  $C_\ell(\alpha_m)$  is very close to unity for all relevant  $\alpha_m$ , the results are indistinguishable from those obtained using the single-mode approximation of Ref. [15]. We mention that our numerical results differ slightly from those in Ref. [15], with more clearly visible peaks up to larger harmonic numbers. This is most likely due to our use of a smooth cutoff of the dipole acceleration in time after the end of the pulse, which reduces numerical artifacts in the Fourier transform due to dipole oscillations between bound states that otherwise persist after the end of the pulse (infinitely if spontaneous emission is not taken into account).

The resulting spectra are indistinguishable for Fock and coherent states, since their Husimi distributions are very narrowly peaked around the mean intensity. In contrast, thermal and BSV states give significantly higher HHG yields due to their much broader intensity distributions. Based on the resulting emission spectrum, us-

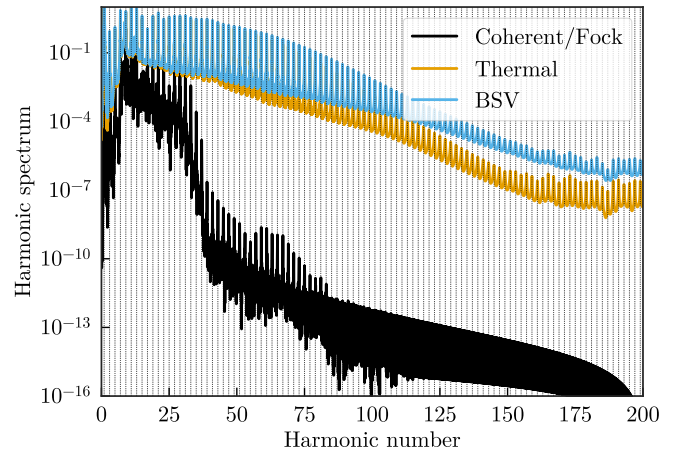


FIG. 4. Harmonic spectrum of the different light distributions for a constant mean intensity. The peaks at odd multiples of the driving frequency  $\omega_0$  arise because the electric field  $E_\alpha(t)$  reaches a maximum (in absolute value) every half cycle.

ing thermal or BSV states instead of coherent or Fock states may appear more advantageous for generating high-harmonic pulses.

However, these differences do not represent genuine quantum effects. While in principle the Husimi distribution is unique (i.e., the full quantum state can be reconstructed from it, which in turn means that two Husimi distributions are only identical if they describe the same exact density matrix), the fact that it is a real and positive quantity means that any sufficiently broad distribution can be reasonably approximated by an incoherent sum over unit-width Gaussians (i.e., coherent states). Such a Husimi function corresponds to a classical statistical sum of coherent (i.e., classical) states and thus cannot show any quantum effects—in other words, the same statistical properties of the light field can be obtained from an average over purely classical fields. Note that the coherent state and thermal distributions already have this property even without any averaging over Gaussians. In contrast, BSV and Fock states are *a priori* “quantum” states.

Even so, a corollary of our result regarding the near-unity value of the correction factor  $C_\ell(\alpha)$  is the explicit confirmation that convolution of the Husimi function with a Gaussian of unit width in  $\alpha$  will not significantly change the HHG spectrum for situations where many photons are required to reach intensities where HHG takes place. This is because the validity of the diagonal approximation implies that the HHG spectrum changes little for variations of  $\alpha$  on the order of unity (note that this is exactly the argument behind the conventional use of the semi-classical approximation in strong-field physics due to the well-known fact that fluctuations in coherent states are negligible for large photon numbers). Nonetheless, such a convolution corresponds to a density matrix that is a classical statistical mixture of coherent states,  $\rho = \int d^2\alpha Q(\alpha) |\alpha\rangle\langle\alpha|$ , and thus cannot show any genuine

quantum effects.

The observed differences in the HHG spectrum between the distinct quantum states of light are thus purely due to the fact that the statistical distribution of the intensities are distinct for different states. In other words, the enhanced HHG yield is simply due to the fact that the “quantum” fields have large fluctuations in intensity for the same average intensity. A classical source of pulses with varying peak intensities would give the same result. Other light states do not possess an inherent advantage, excluding the possibility of non-classical effects under the approximations discussed.

#### IV. CONCLUSIONS

In this work, we have extended the theoretical framework for high-harmonic generation (HHG) driven by quantum states of light from the single plane-wave mode treatment of Ref. [15] to a realistic temporal-mode description. This extension resolves conceptual inconsistencies in the previous treatment by removing the dependence on an infinitely extended, non-normalizable plane wave and bringing the analytical framework into full agreement with numerical simulations employing finite pulses.

We have shown that the temporal-mode expansion introduces a correction factor  $C_\ell(\alpha_m)$  to the HHG spectrum. For peak intensities of  $I_{\text{HHG}} \sim 10^{14}$  W/cm<sup>2</sup> typical of HHG experiments, this correction factor deviates from unity by less than  $10^{-4}$  across the entire HHG spectrum, validating the diagonal approximation and confirming the accuracy of the single-mode result for HHG driven by pulses in arbitrary quantum states in free space.

Our results demonstrate that the HHG spectrum can be computed by averaging semi-classical calculations over the Husimi quasi-probability distribution  $Q(\alpha)$  of the driving field. The validity of the diagonal approximation implies that convolving this distribution with a Gaussian of unit width in  $\alpha$  does not significantly change the HHG spectrum. Since such a convolution corresponds to a classical statistical mixture of coherent states, genuine quantum effects cannot be observed in HHG under these conditions. The enhanced yield observed for states such as bright squeezed vacuum arises purely from their broader statistical distribution of peak intensities, not from quantum effects. A classical ensemble of pulses with the same intensity distribution would produce identical results.

The fundamental reason for the absence of quantum effects in free-space HHG is the requirement of large photon numbers ( $|\alpha_m|^2 \sim 10^{11}$ ). Under such conditions, quantum fluctuations  $\delta\alpha \sim 1$  are negligible compared to  $\alpha_m \sim 10^5$ , and the diagonal approximation becomes exact. However, in nanophotonic environments with ultrasmall mode volumes ( $V \sim 1$  nm<sup>3</sup>), reaching HHG intensities would require only  $\sim 10$  photons. In such few-photon regimes, the diagonal approximation breaks

down, and genuine quantum effects could potentially manifest, opening new directions for exploring quantum strong-field physics at the intersection of quantum optics and attosecond science.

#### ACKNOWLEDGMENTS

This work was funded by the Spanish Ministry of Science, Innovation and Universities-Agencia Estatal de Investigación through Grants PID2021-125894NB-I00, CNS2023-145254, PID2024-161142NB-I00 and CEX2023-001316-M (through the María de Maeztu program for Units of Excellence in R&D). We also acknowledge financial support from the European Union’s Horizon Europe Research and Innovation Programme through grant agreement 101070700 (MIRAQLS).

#### Appendix A: Derivation of Schrödinger Equation

The general solution of the von Neumann equation, Eq. (9), may be formally written with the time-evolution operator  $U(t)$

$$\begin{aligned}\rho_{\alpha\beta}(t) &= U(t)\rho_{\alpha\beta}(0)U^\dagger(t), \\ U(t) &= \mathcal{T}e^{-\frac{i}{\hbar}\int_0^t d\tau \hat{H}_o(\tau)},\end{aligned}\tag{A1}$$

with  $\mathcal{T}$  being the time-ordering operator. It is now convenient to introduce coherent displacement operators  $D(\alpha)$ . The operator shifts the vacuum state  $|0\rangle$  to a coherent state described by the argument parameter, in this case  $|\alpha\rangle$ ,  $D(\alpha)|0\rangle = |\alpha\rangle$ . With shift operators we may rewrite  $\rho_{\alpha\beta}(0)$  as  $\rho_{\alpha\beta}(0) = |g\rangle\langle g| \otimes D(\alpha) \prod_\nu |0_\nu\rangle\langle 0_\nu| D^\dagger(\beta)$ . Additionally, a new operator  $\tilde{\rho}_{\alpha\beta}(t)$  can be defined as  $\tilde{\rho}_{\alpha\beta}(t) = D^\dagger(\alpha)\rho_{\alpha\beta}(t)D(\beta)$ , given explicitly by

$$\begin{aligned}\tilde{\rho}_{\alpha\beta}(t) &= [D^\dagger(\alpha)U(t)D(\alpha)]|g\rangle\langle g| \otimes \\ &\otimes \prod_\nu |0_\nu\rangle\langle 0_\nu| [D^\dagger(\beta)U(t)D(\beta)]^\dagger.\end{aligned}\tag{A2}$$

This operator can be expressed as  $\tilde{\rho}_{\alpha\beta}(t) = |\psi_\alpha(t)\rangle\langle\psi_\beta(t)|$  by defining

$$|\psi_\alpha(t)\rangle = [D^\dagger(\alpha)U(t)D(\alpha)]|g\rangle \otimes \prod_\nu |0_\nu\rangle,\tag{A3}$$

which allows us to rewrite Eq. (10) as

$$\rho(t) = \int d^2\alpha d^2\beta \frac{P(\alpha, \beta^*)}{\langle\beta|\alpha\rangle} D(\alpha)|\psi_\alpha(t)\rangle\langle\psi_\beta(t)| D^\dagger(\beta).\tag{A4}$$

The trace of  $\rho(t)$  can be checked to be equal to 1, as is necessary for probability to be conserved.

Using Eqs. (A2) and (A3), Eq. (9) can be expressed as

$$\begin{aligned}i\hbar\frac{\partial}{\partial t} (D(\alpha)|\psi_\alpha(t)\rangle\langle\psi_\beta(t)| D^\dagger(\beta)) &= \\ &= [H_o(t), D(\alpha)|\psi_\alpha(t)\rangle\langle\psi_\beta(t)| D^\dagger(\beta)].\end{aligned}\tag{A5}$$



After operating, we find that  $|\psi_\alpha(t)\rangle$  satisfies the Schrödinger equation

$$i\hbar \frac{\partial |\psi_\alpha(t)\rangle}{\partial t} = D^\dagger(\alpha) H_o(t) D(\alpha) |\psi_\alpha(t)\rangle, \quad (\text{A6})$$

and so does  $|\psi_\beta(t)\rangle$  under the replacement  $\alpha \rightarrow \beta$ . Inserting  $H_o(t) = H_A(t) + \vec{d} \cdot \vec{E}(x, t)$ , we can use the fact that the displacement operators do not act on the atomic Hamiltonian  $H_A(t)$ , and that they are unitary  $D(\alpha) D^\dagger(\alpha) = 1$ , to show that only the second term is affected. The dipole operator  $\vec{d}$  remains unchanged as it is an atomic operator, but the displacement operators do act on the electric field  $\vec{E}(x, t)$ . Using the properties  $D^\dagger(\alpha) a D(\alpha) = a + \alpha$ , and  $D^\dagger(\alpha) a^\dagger D(\alpha) = a^\dagger + \alpha^*$ , we get that

$$D^\dagger(\alpha) \vec{E}(x, t) D(\alpha) = \vec{E}(x, t) + \vec{E}_\alpha(x, t). \quad (\text{A7})$$

This way, we can rewrite Eq. (A6) with a “new” Hamiltonian which will have two contributions. The first contribution will be the quantized electric field, and the new term which appears is that of a classical field.

$$i\hbar \frac{\partial |\psi_\alpha(t)\rangle}{\partial t} = H_\alpha(t) |\psi_\alpha(t)\rangle, \quad (\text{A8})$$

$$H_\alpha(t) = H_A + \vec{d} \cdot \vec{E} + \vec{d} \cdot \vec{E}_\alpha(t),$$

with initial condition  $|\psi_\alpha(0)\rangle = |g\rangle \otimes \prod_\nu |0_\nu\rangle$ . We will write the solution as a product of coherent states, supposing there isn't any overlap between the light states and atom. Therefore, we may write it as tensor product, as described starting from Eq. (12) in the main text.

## Appendix B: Fourier Transform of the Electric Field

In order to simplify the second term in the exponential of the expression for the correction factor in Eq. (28), we consider the electric field, evaluated at  $\vec{r} = 0$  in the new basis with the coefficients  $c_\ell$  of the unitary transformation:

$$\vec{E}(\vec{r} = 0, t) = \sum_\ell (\vec{f}_\ell(0, t) c_\ell b + \text{H.c.}). \quad (\text{B1})$$

The polarization vector  $\vec{e}_\sigma = \hat{x}$  has been chosen as fixed, since the field is propagating along the z-axis. Taking the continuum limit of infinite quantization volume  $V \rightarrow \infty$  gives:

$$\vec{E}(0, t) = \frac{V}{(2\pi)^3 c^3} \sum_\sigma \int_0^\infty d\omega \omega^2 \int d\Omega$$

$$\left( \vec{f}_\ell(0, t) c(\omega, \Omega, \sigma) b + \text{H.c.} \right). \quad (\text{B2})$$

We next take the expectation value, which corresponds to the substitution  $b \rightarrow \alpha$

$$\langle \vec{E}(0, t) \rangle = \frac{V}{(2\pi)^3 c^3} \sum_\sigma \int_0^\infty d\omega \omega^2 \int d\Omega$$

$$\left( \vec{f}_\ell(0, t) c(\omega, \Omega, \sigma) \alpha + \text{H.c.} \right). \quad (\text{B3})$$

Continuing from this last expression we write  $\vec{f}_\ell(0, t) = i\epsilon^{(1)} e^{-i\omega t} \vec{e}_\sigma$  to explicitly show the time dependence, and we take the (unitary) Fourier transform to obtain the frequency distribution of the field

$$\mathcal{F}[\langle \vec{E}(0, t) \rangle] = \langle \vec{E}(\omega') \rangle =$$

$$= \frac{V}{(2\pi)^3 c^3} \sum_\sigma \int_0^\infty d\omega \omega^2 \int d\Omega i\epsilon^{(1)} c(\omega, \Omega, \sigma) \alpha \vec{e}_\sigma$$

$$+ \int_{-\infty}^{+\infty} dt \frac{e^{i(\omega' - \omega)t}}{\sqrt{2\pi}} - \frac{V}{(2\pi)^3 c^3} \sum_\sigma \int_0^\infty d\omega \omega^2$$

$$\int d\Omega i\epsilon^{(1)} c^*(\omega, \Omega, \sigma) \alpha^* \vec{e}_\sigma \int_{-\infty}^{+\infty} dt \frac{e^{i(\omega' + \omega)t}}{\sqrt{2\pi}}. \quad (\text{B4})$$

Applying a Fourier transform identity for the delta function,  $\int_{-\infty}^{+\infty} dt e^{i(\omega' - \omega)t} = 2\pi \delta(\omega' - \omega)$ , we obtain

$$\mathcal{F}[\langle \vec{E}(0, t) \rangle] = \langle \vec{E}(\omega') \rangle =$$

$$= \sqrt{2\pi} \frac{V}{(2\pi)^3 c^3} \sum_\sigma \int d\Omega i\epsilon^{(1)} \omega'^2 c(\omega', \Omega, \sigma) \alpha \vec{e}_\sigma -$$

$$- \sqrt{2\pi} \frac{V}{(2\pi)^3 c^3} \sum_\sigma \int d\Omega i\epsilon^{(1)} \omega'^2 c^*(-\omega', \Omega, \sigma) \alpha^* \vec{e}_\sigma$$

$$= \langle \vec{E}^+(\omega') \rangle + \langle \vec{E}^-(\omega') \rangle. \quad (\text{B5})$$

We have now two different contributions to the Fourier transform, one with positive frequencies and a second with negative frequencies. They satisfy the relation  $\vec{E}^+(\omega') = \vec{E}^{*-}(-\omega')$ , which ensures that  $\vec{E}(0, t)$  is real. These positive and negative frequency terms will be related to the second term of the exponential, which is presented again here for clarity:

$$\frac{1}{\hbar} \int d\omega \frac{V}{(2\pi)^3 c^3} \sum_\sigma \int d\Omega i\epsilon^{(1)} \omega^2 c^*(\omega, \Omega, \sigma) \alpha^* \vec{e}_\sigma$$

$$\cdot (\vec{d}_\alpha(\omega) - \vec{d}_\beta(\omega)) + \frac{1}{\hbar} \int d\omega \frac{V}{(2\pi)^3 c^3} \sum_\sigma$$

$$\int d\Omega i\epsilon^{(1)} \omega^2 c(\omega, \Omega, \sigma) \beta \vec{e}_\sigma \cdot (\vec{d}_\alpha^*(\omega) - \vec{d}_\beta^*(\omega)). \quad (\text{B6})$$

It can be noticed that, save some prefactors inside the integral, the elements are just the expression of the Fourier transform of the electric field obtained in Eq. (B5). As such, the integral can be rewritten in terms of the scalar product of the electric field with dipole moments.

$$-\frac{1}{\hbar \sqrt{2\pi}} \int_0^\infty d\omega \vec{E}_\alpha^-(\omega) \cdot (\vec{d}_\alpha(\omega) - \vec{d}_\beta(\omega)) +$$

$$+ \frac{1}{\hbar \sqrt{2\pi}} \int_0^\infty d\omega \vec{E}_\beta^+(\omega) \cdot (\vec{d}_\alpha^*(\omega) - \vec{d}_\beta^*(\omega)), \quad (\text{B7})$$

where  $\vec{E}^-(\omega)$  and  $\vec{E}^+(\omega)$  are the negative and positive frequency Fourier transform of the complete electric field, respectively. As  $\vec{E}(0, t)$  is real, as mentioned previously  $\vec{E}^-(\omega) = \vec{E}^{+*}(\omega)$  and thus the term is finally written as

$$\begin{aligned} & \frac{-1}{\hbar\sqrt{2\pi}} \int_0^\infty d\omega \vec{E}_\alpha^{+*}(\omega) \cdot (\vec{d}_\alpha(\omega) - \vec{d}_\beta(\omega)) + \\ & + \frac{1}{\hbar\sqrt{2\pi}} \int_0^\infty d\omega \vec{E}_\beta^+(\omega) \cdot (\vec{d}_\alpha^*(\omega) - \vec{d}_\beta^*(\omega)). \end{aligned} \quad (\text{B8})$$

### Appendix C: Normalization of field

We here discuss how to normalize the electric field for a temporal mode with a given temporal shape. From Ref. [29], a transversal field that is confined within a cross-sectional area  $A$  but extends to infinity along one axis, with a certain polarization, may be expressed as

$$E_{1,p}^+(x, t) = i \int_0^\infty d\omega \left( \frac{\hbar\omega}{4\pi\epsilon_0 cA} \right)^{1/2} c(\omega) e^{-i\omega(t - \frac{x}{c})}, \quad (\text{C1})$$

where we emphasize the subindex 1 to make clear that this is the quantized field of a single photon, and correct normalization requires  $\int_0^\infty d\omega |c(\omega)|^2 = 1$ . Since we are only interested in  $x = 0$  we can evaluate it at that particular  $x$  and have it be a function of time only. Writing the field as an inverse Fourier transform gives

$$\begin{aligned} E_{1,p}^+(0, t) &= i \int_0^\infty d\omega \left( \frac{\hbar\omega}{4\pi\epsilon_0 cA} \right)^{1/2} c(\omega) e^{-i\omega t} = \\ &= \frac{1}{\sqrt{2\pi}} \int_0^\infty d\omega \tilde{E}_{1,p}^+(\omega) e^{-i\omega t}, \end{aligned} \quad (\text{C2})$$

establishing the relation  $c(\omega) = -i\tilde{E}_{1,p}^+(\omega) \left( \frac{2\epsilon_0 cA}{\hbar\omega} \right)^{1/2}$ . The normalization of  $c(\omega)$  then requires solution of the integral  $\int_0^\infty d\omega \frac{|\tilde{E}^+(\omega)|^2}{\omega}$ , which for the flat-top laser pulse considered in this work, given by Eq. (33), can be expressed as  $\frac{E_{1,p}^2}{\omega_0^2} \mathcal{I}(n_r, n_f)$ , where  $\mathcal{I}(n_r, n_f)$  is a unitless normalization integral whose value depends on the number of laser cycles in the ramp-on ( $n_r$ ) and constant ( $n_f$ ) parts of the pulse. Although it can be solved analytically for integer values of  $n_r$  and  $n_f$ , the expression is quite lengthy and not given here for conciseness. For the values used in this work,  $n_r = 5$  and  $n_f = 15$ , we find  $\mathcal{I}(5, 15) \approx 28.814$ . We note that the specific pulse shape chosen is only normalizable for integer values of  $n_r$  and  $n_f$ , indicating that it does not correspond to a physical pulse propagating in free space for other values of these parameters. This is because it would break the condition that the value of the vector potential is the same before and after the pulse that is required for propagating pulses. Using this integral, we obtain the electric field amplitude  $E_{1,p}$  of the quantized temporal mode, as given in Eq. (34),

$$E_{1,p} = \sqrt{\frac{\hbar\omega_0}{2\epsilon_0 V_{\text{eff}}}}, \quad (\text{C3})$$

where  $V_{\text{eff}} = n_{\text{eff}} A \lambda_0$  is an effective mode volume, with  $n_{\text{eff}} = \frac{2}{\pi} \mathcal{I}(n_r, n_f) \approx 18.343$  being the effective number of cycles in the pulse. Note that  $n_{\text{eff}}$  is close to, but not exactly equal to  $n_f + \frac{2}{3}n_r = 18.333$ , the value that would be obtained when replacing  $\omega \rightarrow \omega_0$  in the denominator of the normalization integral.

- 
- [1] I. A. Gonoskov, N. Tsatrafyllis, I. K. Kominis, and P. Tzallas, Quantum optical signatures in strong-field laser physics: Infrared photon counting in high-order harmonic generation, *Sci. Rep.* **6**, 32821 (2016).
  - [2] A. Gorlach, O. Neufeld, N. Rivera, O. Cohen, and I. Kaminer, The quantum-optical nature of high harmonic generation, *Nature Communications* **11**, 4598 (2020).
  - [3] Á. Gombkötő, P. Földi, and S. Varró, Quantum-optical description of photon statistics and cross correlations in high-order harmonic generation, *Phys. Rev. A* **104**, 033703 (2021).
  - [4] M. E. Tzur, M. Birk, A. Gorlach, M. Krüger, I. Kaminer, and O. Cohen, Photon-statistics force in ultrafast electron dynamics, *Nat. Photonics* **17**, 501 (2023).
  - [5] P. Stammer, J. Rivera-Dean, A. Maxwell, T. Lamprou, A. Ordóñez, M. F. Ciappina, P. Tzallas, and M. Lewenstein, Quantum Electrodynamics of Intense Laser-Matter Interactions: A Tool for Quantum State Engineering, *PRX Quantum* **4**, 010201 (2023).
  - [6] I. Gonoskov, R. Sondenheimer, C. Hünecke, D. Kartashov, U. Peschel, and S. Gräfe, Nonclassical light generation and control from laser-driven semiconductor intraband excitations, *Phys. Rev. B* **109**, 125110 (2024).
  - [7] S. Yi, N. D. Klimkin, G. G. Brown, O. Smirnova, S. Patchkovskii, I. Babushkin, and M. Ivanov, Generation of Massively Entangled Bright States of Light during Harmonic Generation in Resonant Media, *Phys. Rev. X* **15**, 011023 (2025).
  - [8] N. Tsatrafyllis, I. K. Kominis, I. A. Gonoskov, and P. Tzallas, High-order harmonics measured by the photon statistics of the infrared driving-field exiting the atomic medium, *Nat. Commun.* **8**, 15170 (2017).
  - [9] M. Lewenstein, M. F. Ciappina, E. Pisanty, J. Rivera-Dean, P. Stammer, Th. Lamprou, and P. Tzallas, Generation of optical Schrödinger cat states in intense laser-matter interactions, *Nature Physics* **17**, 1104 (2021).
  - [10] D. Theidel, V. Cotte, R. Sondenheimer, V. Shiraeva, M. Froidevaux, V. Severin, A. Merdji-Larue, P. Mosel, S. Fröhlich, K.-A. Weber, U. Morgner, M. Kovacev, J. Biegert, and H. Merdji, Evidence of the Quantum Optical Nature of High-Harmonic Generation, *PRX Quantum* **5**, 040319 (2024).
  - [11] D. Theidel, V. Cotte, P. Heinzel, H. Griguer, M. Weis, R. Sondenheimer, and H. Merdji, Observation of a displaced squeezed state in high-harmonic generation, *Phys.*

- [Rev. Res. \*\*7\*\*, 033223 \(2025\)](#).
- [12] T. Iskhakov, M. V. Chekhova, and G. Leuchs, Generation and Direct Detection of Broadband Mesoscopic Polarization-Squeezed Vacuum, [Phys. Rev. Lett. \*\*102\*\*, 183602 \(2009\)](#).
  - [13] K. Yu. Spasibko, T. Sh. Iskhakov, and M. V. Chekhova, Spectral properties of high-gain parametric down-conversion, [Opt. Expr. \*\*20\*\*, 7507 \(2012\)](#).
  - [14] M. Chekhova, G. Leuchs, and M. Żukowski, Bright squeezed vacuum: Entanglement of macroscopic light beams, [Opt. Commun. \*\*337\*\*, 27 \(2015\)](#).
  - [15] A. Gorlach, M. E. Tzur, M. Birk, M. Krüger, N. Rivera, O. Cohen, and I. Kaminer, High-harmonic generation driven by quantum light, [Nature Physics \*\*19\*\*, 1689 \(2023\)](#).
  - [16] A. Rasputnyi, Z. Chen, M. Birk, O. Cohen, I. Kaminer, M. Krüger, D. Seletskiy, M. Chekhova, and F. Tani, High-harmonic generation by a bright squeezed vacuum, [Nat. Phys. \*\*20\*\*, 1960 \(2024\)](#).
  - [17] H. Liu, H. Zhang, X. Wang, and J. Yuan, Atomic Double Ionization with Quantum Light, [Phys. Rev. Lett. \*\*134\*\*, 123202 \(2025\)](#).
  - [18] G. Mouloudakis and P. Lambropoulos, Revisiting photon-statistics effects on multiphoton ionization, [Phys. Rev. A \*\*97\*\*, 053413 \(2018\)](#).
  - [19] G. Mouloudakis and P. Lambropoulos, Revisiting photon-statistics effects on multiphoton ionization. II. Connection to realistic systems, [Phys. Rev. A \*\*99\*\*, 063419 \(2019\)](#).
  - [20] S. Lemieux, S. A. Jalil, D. N. Purschke, N. Boroumand, T. J. Hammond, D. Villeneuve, A. Naumov, T. Brabec, and G. Vampa, Photon bunching in high-harmonic emission controlled by quantum light, [Nat. Photonics \*\*19\*\*, 767 \(2025\)](#).
  - [21] M. E. Tzur, C. Mor, N. Yaffe, M. Birk, A. Rasputnyi, O. Kneller, I. Nisim, I. Kaminer, M. Krüger, N. Dudovich, and O. Cohen, Measuring and controlling the birth of quantum attosecond pulses, [arXiv:2502.09427 \[physics\] \(2025\)](#).
  - [22] J. Feist, A. I. Fernández-Domínguez, and F. J. García-Vidal, Macroscopic QED for quantum nanophotonics: emitter-centered modes as a minimal basis for multiemitter problems, [Nanophotonics \*\*10\*\*, 477 \(2021\)](#).
  - [23] S. Y. Buhmann, [Dispersion Forces I](#), Springer Tracts in Modern Physics, Vol. 247 (Springer Berlin Heidelberg, Berlin, Heidelberg, 2012).
  - [24] B. Brecht, D. V. Reddy, C. Silberhorn, and M. G. Raymer, Photon Temporal Modes: A Complete Framework for Quantum Information Science, [Phys. Rev. X \*\*5\*\*, 041017 \(2015\)](#).
  - [25] P. D. Drummond and C. W. Gardiner, Generalised P-representations in quantum optics, [Journal of Physics A: Mathematical and General \*\*13\*\*, 2353 \(1980\)](#).
  - [26] W. Li, Q. Zhou, P. Zhang, and X.-W. Chen, Bright Optical Eigenmode of  $1 \text{ nm}^3$  Mode Volume, [Phys. Rev. Lett. \*\*126\*\*, 257401 \(2021\)](#).
  - [27] T. Wu, W. Yan, and P. Lalanne, Bright Plasmons with Cubic Nanometer Mode Volumes through Mode Hybridization, [ACS Photonics \*\*8\*\*, 307 \(2021\)](#).
  - [28] M. Kim, F. De Oliveira, and P. Knight, Properties of squeezed number states and squeezed thermal states, [Physical Review A \*\*40\*\*, 2494 \(1989\)](#).
  - [29] K. Blow, R. Loudon, S. J. Phoenix, and T. Shepherd, Continuum fields in quantum optics, [Physical Review A \*\*42\*\*, 4102 \(1990\)](#).